RHIC PROJECT

Brookhaven National Laboratory

Transverse Phase Space Reconstruction
of the RHIC Beam

Roger Connolly

February 1999

Transverse Phase Space Reconstruction of the RHIC Beam

Roger Connolly

INTRODUCTION

Transverse beam profiles in the Relativistic Heavy Ion Collider (RHIC) will be measured with ionization beam profile monitors (IPM's) [1]. Each IPM will measure single-bunch profiles of gold beams with intensities of 5-10 x 10^8 ions per bunch. The two-dimensional transverse phase space of the bunch rotates by the fractional tune during each orbit. A set of profiles taken on consecutive turns can be used to reconstruct the phase-space distribution of the bunch by tomographic techniques [2,3,4,].

This paper describes the filtered back-projection reconstruction method. Conventionally this technique is used with projection sets of the measured object taken by incrementing the projection angle in small constant steps between 0 and 180°. In RHIC the transverse phase space of the beam rotates between measurements by angles on the order of 65-70°. A simulation was written in Labview to investigate the dependance of reconstruction resolution on the number of samples taken, the fractional tune, and system noise.

FILTERED BACK PROJECTION RECONSTRUCTION

Central section theorem

The method of filtered back projection reconstruction is described here [5]. Tomographic reconstruction techniques were developed for x-ray imaging applications. In x-ray imaging the contrast mechanism is signal attentuation by absorbing material. For beam measurements the contrast mechanism is the distribution of electrons separated from background gas atoms by the ionizing beam particles. Beam measurements are made with a fixed detector and the measured distribution rotates between measurements by the fractional tune, q, times 2. First the more conventional technique of rotating a detector around a fixed distribution will be described.

Consider a signal-generating two-dimensional distribution f(x,y) as shown in fig. 1. Here f(x,y) is the signal-generating strength per unit area in the fixed reference frame. A detector is employed which projects all of the generated signal from the distribution in a single direction. In x-ray tomography this is done with pencil beams. For the IPM the external magnetic field constrains the signal electrons to move perpendicular to the multi-anode collector. The signal is extracted from the distribution parallel to the Y_{rot} axis where (X_{rot}, Y_{rot}) is rotated with respect to (x,y) by the angle .
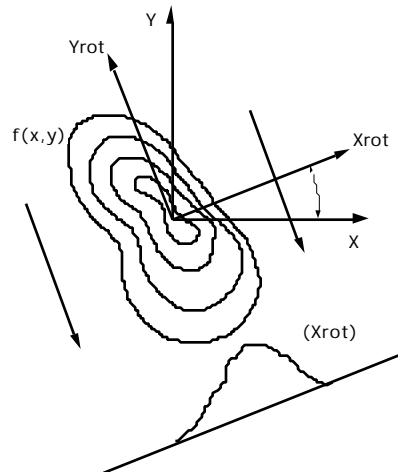
Figure 1.   Measurement of a fixed distribution by a rotating detector.

The measured one-dimensional projection distribution, (x_{rot}), is,

$$(x_{rot}) = \int f(x, y)\, dy_{rot} \tag{1}$$

The two-dimensional Fourier transform of $f(x,y)$ is $F(\ ,\ )$ where,

$$F(\ ,\ ) = \frac{1}{2} \int f(x, y)\exp\big(-2\, i[x\ + y\ ]\big)\,dx\,dy \tag{2}$$

It is convenient to write this transform in polar coordinates where,

$$F^{p}(\ ,\ ) = F(\ \cos\ ,\ \sin\ ) \tag{3}$$

If the Fourier transform of the measured projection is $(\ )$, then the central-section theorem states that,

$$(\ ) = F^{p}(\ ,\ ) \tag{4}$$

The one-dimensional Fourier transform of the projection data taken at angle is equal to the value of the two-dimensional Fourier transform of the distribution along the line which passes through the origin at angle . If an infinite number of projections between =0 and = are taken with a detector with infinitesimal resolution, $F(\ ,\ )$ can be fully constructed and $f(x,y)$ can be recovered.

Convolution and backprojection

The inverse Fourier transform to reconstruct the original distribution is,

$$f(x, y) = \frac{1}{2} \int F(\ ,\ )\exp\big(2\, i[x\ + y\ ]\big)\,d\ d$$

$$= \frac{1}{2} \int_{0\ -}^{\ } F^{p}(\ ,\ )\exp\big(2\, i\ (x\cos\ + y\sin\ )\big)\,|\ |\,d\ d \tag{5}$$

Equation 5 can be broken into two parts. First notice that $X_{rot} = x\cos\ + y\sin\ $. Therefore,

$$f(x, y) = \frac{1}{2} \int_{0}^{\ } {}^{f}(x_{rot})\,d\ \Big|_{x_{rot} = x\cos\ + y\sin\ } \tag{6}$$

$${}^{f}(x_{rot}) = \int_{-}^{\ } F^{p}(\ ,\ )\,|\ |\exp\big(2\, i\ x_{rot}\big)\,d \tag{7}$$

Equation 7 is the inverse Fourier transform of the product of two functions. It therefore can be written as the convolution of the inverse transforms of $F^{p}(\ ,\ )$ and $|\ |$. The first function, $F^{p}(\ ,\ )$, is the Fourier transform of the projection data, eqn. 4, so its inverse is simply the measured projection, (X_{rot}).

3

The coordinate, ν, measures spatial frequency. However due to the finite spacing of the collector channels there is an upper cutoff, ν_{max}, above which the integral can be truncated. If we define a function $P(\nu)$,

$$P(\nu) = 0 \qquad\qquad |\nu| > \nu_{max} \tag{8}$$

$$P(\nu) = |\nu| \qquad\qquad |\nu| \le \nu_{max}$$

then the transform of $P(\nu)$ is $p(x_{rot})$ where,

$$p(x_{rot}) = \nu_{max}^2 \left[2\,\mathrm{sinc}\left(2\nu_{max}x_{rot}\right) - \mathrm{sinc}^2\left(\nu_{max}x_{rot}\right) \right] \tag{9}$$

Using the convolution theorem eqn. 7 can now be written,

$$\Lambda^f\!\left(x_{rot}\right) = \int \Lambda(x)\,p\!\left(x_{rot} - x\right)dx \tag{10}$$

The convolution is a filtering operation and the quantity $\Lambda^f\!\left(x_{rot}\right)$ is called a filtered projection. The expression in eqn. 9, graphed in fig. 2, is the Ramachandran-Lakshminarayan filter [6]. This is a low-pass filter which cuts off at ν_{max}. Other filters have been used which reduce the the high-frequency components in the image for noise reduction [7]. Only the filter given by eqn. 9 has been used here.

$$\frac{p(x_{rot})}{\nu_{max}^2}$$
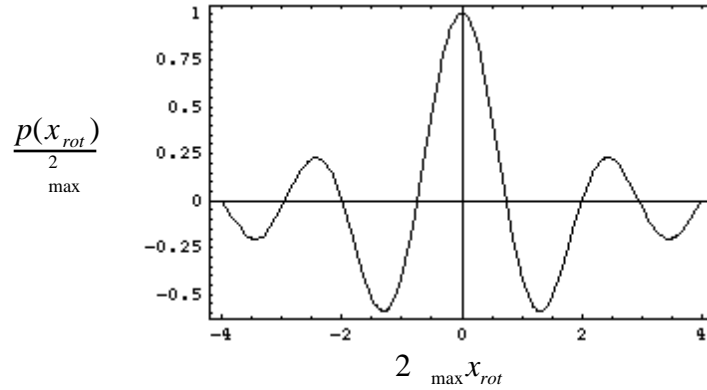
$$2\nu_{max}x_{rot}$$

Figure 2.   The filter function that is convolved with the measured projection to produce a filtered projection.

The final step in reconstruction of the distribution as given by eqn. 6 is *backprojection*. At each angle, ϕ, the filtered projection is dragged over the x,y plane parallel to the Y_{rot} axis. To every point in the x,y plane the value of $\Lambda^f\!\left(x_{rot}\right)$ is added to the current value. The integration over ϕ, is done by adding backprojections from as many angles as possible.

4

Implementation for RHIC

Each RHIC IPM has 64 anode channels and the projection angle between data sets increments by $2\pi q$ where q is the fractional tune. Every measured projection is a set of 64 numbers equally spaced along X_{rot}. The channel spacing, w, determines the largest spatial frequency of $\omega_{max}=(2w)^{-1}$. Since the channels are a fixed distance apart, $w=(2\omega_{max})^{-1}$, eqn. 9 only has to be evaluated at values of $X_{rot}=nw$. The function $p(x_{rot})$ becomes a one-dimensional array,

$$p(nw) = 0 \qquad\qquad\qquad n \text{ even}, n \neq 0$$

$$p(nw) = -(\pi nw)^{-2} \qquad\qquad n \text{ odd} \qquad\qquad\qquad (11)$$

$$p(nw) = (2w)^{-2} \qquad\qquad\qquad n = 0$$

This array is numerically convolved with the projection data resulting in a discrete filtered projection data set.

To reconstruct, we define a 64x64 reconstruction array with pixel spacing equal to the collector channel spacing. The X_{rot} coordinate of the center of each array element is calculated as $X_{rot}=x\cos\theta + y\sin\theta$. An interpolation is done on the filtered projection data to find the value at X_{rot} and this value is added to the pixel. This process is repeated for each measured set building up a reconstruction.

LABVIEW SIMULATION

A reconstruction simulation was written in Labview [8]. First a distribution, $f(x,y)$, is defined. The values of this function are calculated at the centers of a 64x64 grid with the collector spacing. The elements in each column are added to give a measured projection data set. This set is convolved with eqn. 9 and then backprojected as described above.

Several distribution functions were tried. The one that will be discussed is $f=\exp(-r^2)\cos^2$ shown in fig. 3.
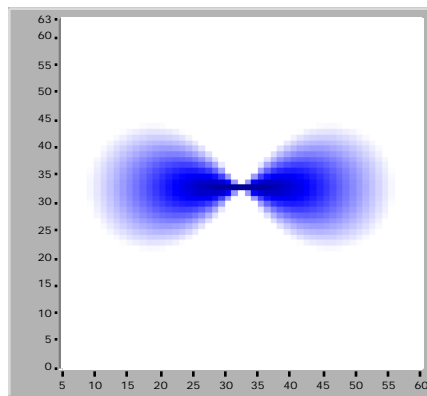

Figure 3.   The two-dimensional array used for reconstruction studies.

Figure 4a shows the reconstruction when the fractional tune is either 0.0 or 0.5. In these two cases the distribution either remains stationary or rotates 180° between measurements. Thus all backprojections are identical and they simply pile up. Figure 4a thus demonstrates a single backprojection. Figure 4b shows the reconstruction when the fractional tune is 0.25. Vertical and horizontal projections are overlaid.
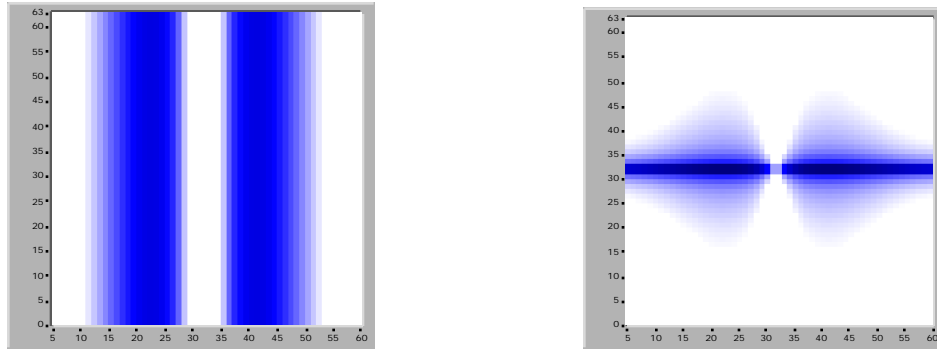
Figure 4.   a. A single backprojection from distribution shown in fig. 3. This would result from q=0 or 0.5. b. Two backprojections from fig. 3, one vertical and one horizontal (q=0.25 or 0.75).

Next we show the results for the RHIC fractional tunes. In Figure 5 the fractional tune is 0.19. The three panels show reconstructions from 20, 30, and 50 projections. These distributions were built up from sequential projections of the parent distribution, fig. 3, by rotating the distribution through an angle of 2 q between measurements. Each projection angle therefore is the accumulated angle modulo 2 . It is not necessary to sort the projection angles or to ensure that the projection angles uniformly cover the interval 0 to or 0 to 2 .
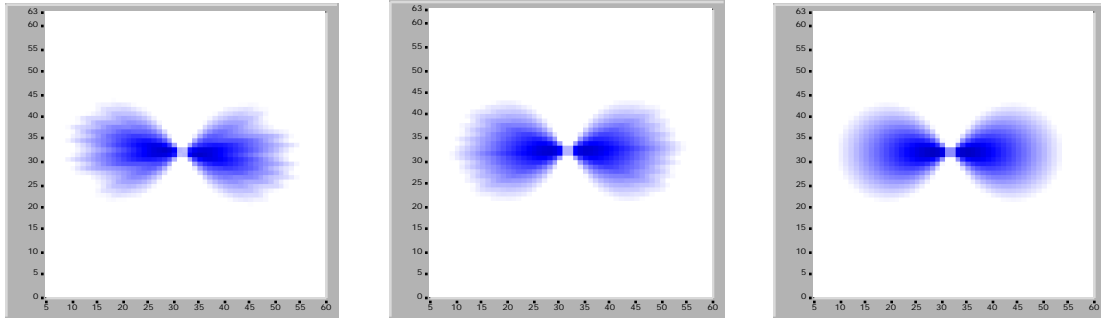

Figure 5.   Reconstructions from 20, 30, and 50 projections. The fractional tune is 0.19.

The reconstruction only works well when the fractional tune is such that there are many projections before the projection angle set starts to repeat. For instance with a fractional tune of 0.17 or 0.19 the projection angles between 0° and 180° repeat after 50 measurements. For q=0.15 the repeat period is 10 turns. Reconstructions from 50 projections for these three fractional tunes are shown in fig 6. The left panel is the result from q=0.15. This gives only ten projections in the range of 0 to resulting in the star-shaped pattern. The center panel is q=0.17 and the right panel is q=0.19.
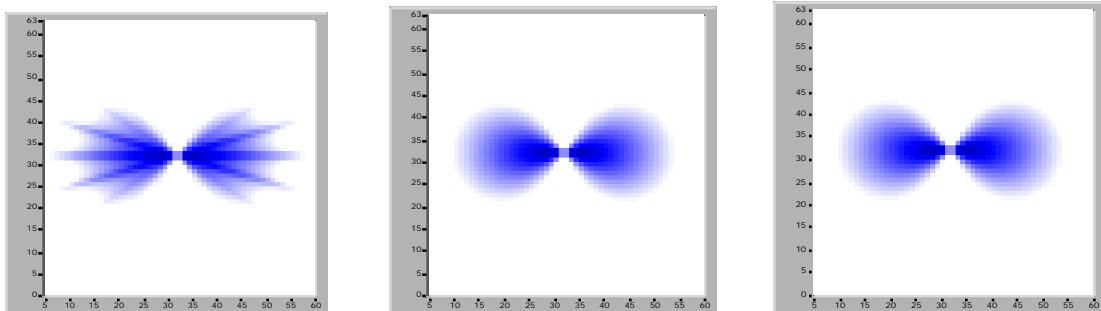

Figure 6.   Reconstructions from 50 projections for q= 0.15, 0.17, 0.19.

6

In all of these reconstructions the projection angle is incremented by the fractional tune and the filtered profile is projected back onto the reconstruction array. This is done sequentially, one projection at a time. There is no need to sort the projection angles into any order. The IPM will capture and store a profile on each turn. Therefore any set of consecutive profiles can be used for reconstruction and evolving phase-space distortions can be studied at several time intervals.

Finally fig. 7 shows the reconstructions with white noise added to the measured projections. The fractional tune is 0.19 and 50 profiles are used. The first plot is with a maximum noise amplitude equal to 10% of the counts in the peak channels and the second is with a noise amplitude of 20%. In these plots the dark corners are an artifact of the signals not being defined beyond the 64 x 64 array. As the parent array rotates the corners of the reconstruction array have no data. As pointed out earlier, these reconstructions are made by applying the Ramachandran-Lakshminarayan filter. Other filters which roll off at lower frequencies might do a better job of filtering noise.
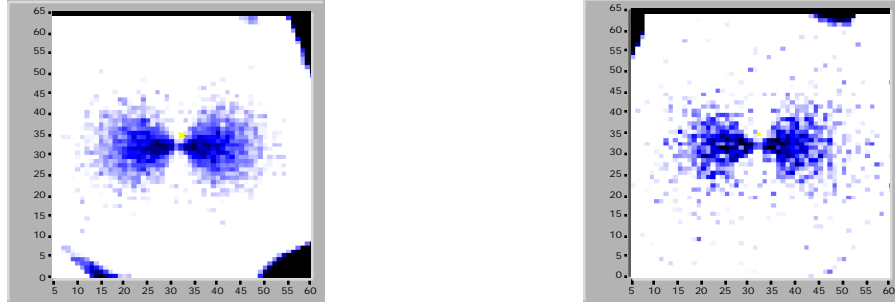

Figure 7.   Reconstructions with noise added to the measured projections. Fifty projections are used with q=0.19. The noise amplitude to peak signal amplitude ratios are 0.10 and 0.20.

TRANSVERSE PHASE SPACE RECONSTRUCTION

The primary use of this technique will be to visualize nonuniformities in the filling of phase space. Such artifacts as filimentation, phase-space holes (from holes in stripper foils for example), or irregular distributions are not apparent from profiles. The following section discusses the cases when the beam uniformly fills phase space and is either matched or has steering or focusing errors.

Matched beam

In normal tomography the distribution which is mapped exists in two spatial coordinates. Phase-space reconstruction, however, involves a two-dimensional distribution in which one of the coordinates, X', is not imaged directly. The projection of the distribution after a 90° phase advance is not a direct measure of the orthogonal dimension.

To first order, at a given location, s, along the beam line a beam particle appears on consecutive passes on an ellipse given by,

$$\gamma_o(s)x^2 + 2\alpha_o(s)xx' + \beta_o(s)x'^2 = C \tag{12}$$

where $\beta_o(s)$, $\alpha_o(s)$ and $\gamma_o(s)$ are the lattice Courant-Snyder parameters. The acceptance, A, of the accelerator is defined as the area of the largest particle orbit which can exist. This trajectory is the machine ellipse and $C=A/\pi$. Each particle travels on its own, smaller ellipse defined by $C=C_p A/\pi$. The beam is matched to the lattice when the beam parameters $\beta_b(s)$, $\alpha_b(s)$ and $\gamma_b(s)$ are equal to the lattice parameters. If the beam uniformly fills phase space, a scatter plot of all the particles' coordinates in phase space forms an ellipse which is concentric and similar to the machine ellipse. Although each particle moves along an elliptical orbit, the projection of the distribution remains constant and the reconstruction will give a circular distribution.

7

In the case of a matched, uniform-density beam, the beam phase space is given by eqn. 12 with $C= \epsilon/\pi$. Here the emittance, ϵ, is defined as the area of the phase space ellipse. The reconstructed circular distribution can be considered to be the phase space of the beam transformed to normalized coordinates (η, ζ) by the Courant-Snyder transformation [9],

$$\begin{pmatrix} \eta \\ \zeta \end{pmatrix} = \begin{pmatrix} \beta^{-\frac{1}{2}} & 0 \\ \alpha\beta^{-\frac{1}{2}} & \beta^{\frac{1}{2}} \end{pmatrix} \begin{pmatrix} X \\ X' \end{pmatrix}$$

(13)

The distribution crosses both the η and ζ axes at $(\epsilon/\pi)^{1/2}$. To transform the reconstructed circular distribution to a representation of the phase space of the beam in conventional coordinates the inverse transformation is applied,

$$\begin{pmatrix} X \\ X' \end{pmatrix} = \begin{pmatrix} \beta^{\frac{1}{2}} & 0 \\ -\alpha\beta^{-\frac{1}{2}} & \beta^{-\frac{1}{2}} \end{pmatrix} \begin{pmatrix} \eta \\ \zeta \end{pmatrix}$$

(14)

From the measured width of the beam, the emittance is calculated from $X_{max}=(\epsilon\beta/\pi)^{1/2}$ and the X' intercept is equal to $(\epsilon\gamma/\pi)^{1/2}$.

Mismatched beam

If there is a steering mismatch the beam profile will be a constant width, but the profile will oscillate transversely at the fractional tune frequency (f_{rev}/q). The reconstruction will produce a circular beam distribution off center. From the tune spread this distribution will spread azimuthally with time. Since the betatron decoherence is on the order of 100-300 turns [10] and adequate distributions can be obtained with 30-50 turns, it should be possible to follow the decoherence process by reconstructing sequential sets of profiles.

A focusing mismatch results in a beam ellipse which is not similar to the machine ellipse. Individual particles however travel on elliptical phase-space trajectories which are similar to the machine ellipse. The result is a small beam ellipse inside of an ellipse similar to the machine ellipse whose orientation rotates on successive turns and whose aspect ratio varies to keep the beam ellipse extremities on the concentric machine ellipse [11]. The reconstruction from the projections will result in an elliptical phase-space reconstruction which is to be compared with the circular reconstruction from the matched beam.

DISCUSSION

The transverse phase space of the RHIC gold beam can be reconstructed from 30-50 individual bunch profiles. Simulations show the reconstruction details start to get washed out if the background noise on the profile measurements gets to be more than about 10% of the peak signal channels. Reconstruction depends on an accurate knowledge of the tune and the method described here assumes the phase space remains constant over the duration of the measurement.

Since any set of consecutive profiles can be used for reconstruction it should be possible to follow phase space changes by using sequential blocks of 30 profiles or by moving a sliding window along the collected profiles. For instance, tune-spread betatron decoherence occurs over a few hundred turns so a 30-profile window should give reasonably good resolution.

ACKNOWLEDGEMENTS

REFERENCES

1. R. Connolly, P. Cameron, W. Ryan, T.J. Shea, R. Sikora, and N. Tsoupas, "A Prototype Ionization Profile Monitor for RHIC", Proceedings of the 1997 Particle Accelerator Conference.
2. V. Yakimenko, M. Babzien, I. Ben-Zvi. R. Malone, S.-.J Wang, "Emittance Control of a Beam by Shaping the Transverse Charge Distribution, Using a Tomography Diagnostic," Proceedings of the 1998 European Particle Accelerator Conference.
3. V. Mane, "Beam Reconstruction in Longitudinal Phase Space," RHIC/AP/96, Brookhaven National Laboratory, Upton, NY 11973.
4. G. Jackson, "Design, Implementation, and Results from a LongitudinalPhase Space Tomography (PST) Monitor in the Fermilab Main Ring," Proceedings of the 1993 Particle Accelerator Conference.
5. A. Kak and M. Slaney, "Principles of Computerized Tomographic Imaging," IEEE Press, New York, 1988.
6. G. Ramachandran and A. Lakshminarayanan, "Three Dimensional Reconstructions from Radiographs and Electron Micrographs: Application of Convolution Instead of Fourier Transforms," Proc. Nat. Acad. Sci., vol. 68, pp. 2236-2240, 1971.
7. L. Shepp and B. Logan, "The Fourier Reconstruction of a Head Section," IEEE Trans. Nucl. Sci., vol. NS-21, pp. 21-43, 1974.
8. LABVIEW, National Instruments, Austin, TX 78730-5039.
9. M. Conte and W. MacKay, "An Introduction to the Physics of Particle Accelerators," p. 84, World Scientific, River Edge, NJ, 1994.
10. R. Connolly, "Decoherence of Betatron Oscillations in RHIC," AD/RHIC/RD-118, Brookhaven National Laboratory, Upton, NY 11973.
11. K. Brown and R. Servranckx, "First- and Second-Order Charged Particle Optics," SLAC-PUB-3381, July 1984, Stanford Linear Accelerator Cernter, Palo Alto, CA.